Author(s): Tatikonda, Rajendhraprasad; Bulatov, Evgeny; Kalenius, Elina; Haukka, Matti

Title: Construction of coordination polymers from semirigid ditopic 2,2´-Biimidazole derivatives : synthesis, crystal structures and characterization

Year: 2017

Version:

Please cite the original version:

Tatikonda, R., Bulatov, E., Kalenius, E., & Haukka, M. (2017). Construction of coordination polymers from semirigid ditopic 2,2´-Biimidazole derivatives : synthesis, crystal structures and characterization. Crystal Growth and Design, 17(11), 5918-5926. https://doi.org/10.1021/acs.cgd.7b01034

Article

Construction of coordination polymers from semi-rigid ditopic 2,2´-Biimidazole derivatives: synthesis, crystal structures and characterization

Rajendhraprasad Tatikonda, Evgeny Bulatov, Elina Kalenius, and Matti Haukka

Cryst. Growth Des., **Just Accepted Manuscript** • DOI: 10.1021/acs.cgd.7b01034 • Publication Date (Web): 03 Oct 2017

Construction of coordination polymers from semi-rigid ditopic 2,2′-biimidazole derivatives: synthesis, crystal structures, and characterization

*Rajendhraprasad Tatikonda, Evgeny Bulatov, Elina Kalenius and Matti Haukka**

Department of Chemistry, University of Jyväskylä, P. O. Box 35, FI-40014 Jyväskylä, Finland.

ABSTRACT: Eight coordination polymers (CPs), $\{[Ag(L1)]ClO_4\}_n$ (**1**), $\{[Ag(L2)_{1.5}]ClO_4 \cdot C_2H_3N\}_n$ (**2a**), $\{[Ag(L2)]ClO_4\}_n$ (**2b**), $[Zn(L1)Cl_2]_n$ (**3**), $\{[Zn(L2)Cl_2] \cdot CHCl_3\}_n$ (**4**), $\{[Cu(L1)_2Cl]Cl \cdot H_2O\}_n$ (**5**), $[Cu_2(L2)(\mu\text{-}Cl)_2]_n$ (**6**) and $[Cu_4(L2)(\mu\text{-}Cl)_4]_n$ (**7**) were synthesized *via* self-assembly of corresponding metal ions and biimidazole based ditopic ligands, 1,1′-bis(pyridin-3-ylmethyl)-2,2′-biimidazole **L1** and 1,1′-bis(pyridin-4-ylmethyl)-2,2′-biimidazole **L2**. These ligands possess conformational flexibility and two pairs of coordination sites: pyridine nitrogen (N_{Py}) atoms and imidazole nitrogen (N_{Im}) atoms. Depending on the metal center in CPs, the biimidazole compounds act as tetra- (**1, 7**), tri- (**2a**) or bidentate (**2a, 2b, 3-6**) ligands binding to the metal either *via* N_{Py} or N_{Im}, or both. All these CPs were structurally fully characterized with single crystal X-ray structure, mass spectrometry, and NMR spectroscopy. The solid state photophysical properties and thermal stabilities of the CPs were also briefly studied in the solid state.

INTRODUCTION

The syntheses of self-assembled coordination polymers (CPs) are receiving growing attention in chemistry as well as in material sciences. Often, CPs are simply obtained by mixing bridging organic ligands and metal ions together. CPs can be tailored to display potential applications in various fields including gas storage,[1-3] nonlinear optics,[4,5] sensing,[6] magnetism,[7,8] catalysis,[9] photocatalysis,[10] and conductivity[11]. Design and production of phosphorescent light emitting devices can also benefit of incorporation of heavy elements into a polymeric chain in coordination polymers.[12] The final structure of CP is dependent on the selection of metal ions, structure of the connecting ligands, possible counter ions, the stoichiometric ratio of the reacting partners, reaction conditions and the solvents used.[13,14] Recently, there has been increasing attention on flexible or semi-rigid ligands particularly a ligand with multiple flexible arms containing several coordination sites.[15-17] Use of semi-rigid ligands in CPs allows the formation of more diverse structures compared to rigid linking ligands. However, it is still possible to design and obtain desired structures with semi-rigid ligands as well. [18,19] In this case, the control of the final structure is often more subtle involving adjustments in reaction conditions. The advance of ligand flexibility is that it can generate completely new properties on CPs. For example, the flexibility of the ligands can be used to produce adaptable cavities within CP structures and enhance properties such as molecular sensing and catalytic activity and selectivity.[20,21]

Over the past few decades, 2,2´-biimidazole (biim) and its derivatives have received much attention due to their versatile chemistry.[22-25] However, construction of novel CPs from

imidazole and biim derivatives is less thoroughly studied.[26,27] With the aim of construction of new CPs, we have chosen two biim derivatives: 1,1′-bis(pyridin-3-ylmethyl)-2,2′-biimidazole (**L1)** and 1,1′-bis(pyridin-4-ylmethyl)-2,2′-biimidazole (**L2)** as the semi-rigid ditopic ligands (Figure 1). The presence of freely rotatable methylene (CH_2) spacer between biim and pyridyl units provides the required flexibility to the ligand. This type of ligands can provide four binding sites: two imidazole nitrogen (N_{Im}) atoms from biim moiety and other two from pyridine nitrogen (N_{Py}) atoms.[28] Coordination ability of N_{Im} and N_{Py} donors is entirely different, which opens up possibilities to control the number of N donors involved in the actual coordination simply by choosing a suitable metal ion.

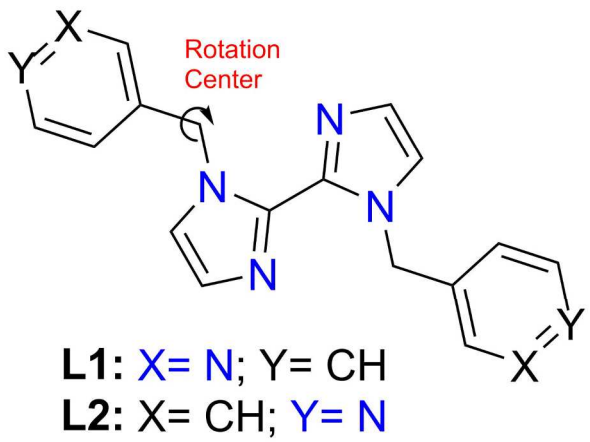

Figure 1. Schematic structure of semi-rigid ligands (**L1** and **L2**) used for the synthesis of CPs.

The ligands (**L1** and **L2**) have been studied as halogen and hydrogen bond acceptors by Aakeröy and co-workers.[29-31] They suggested that the negative electrostatic potentials (NEPs) associated with the pyridine nitrogen atoms (N_{Py}; **L1** = –182 kJ/mol and **L2** = –187 kJ/mol) of both the ligands were proved to be nearly same but higher than the corresponding values of the imidazole nitrogen atoms (N_{Im}; **L1** = –128 kJ/mol and **L2** = –132 kJ/mol) atoms. The higher NEPs of N_{Py} makes them more prone for halogen/hydrogen bonding as well as for metal coordination.

However, there are few reports where N_{Im} coordination was seen along with N_{Py} coordination in the case of **L1**.[32] In acidic reaction conditions, the protonation of N_{Py} atoms directs the ligand towards coordination through N_{Im} atoms.[33]

Choice of the metal ion plays a crucial role in designing CPs due to various electronic structures affecting preferred coordination geometries. In this study, Zn^{2+} was chosen as metal favoring tetrahedral coordination geometry. Copper and silver were selected to provide more flexible coordination geometries. The common geometries of silver(I) complexes are linear, trigonal and tetrahedral.[34-37] Typical coordination geometries of copper(I or II) complexes include tetrahedral, square planar and square pyramidal structures.[38-40]

In this study, we report the synthesis, crystal structures, and characterization of several transition metal (Cu^{+}, Cu^{2+}, Zn^{2+}, and Ag^{+}) coordination polymers with two biim based semi-rigid ligands (**L1** and **L2**), where they act as bi-, tri- or tetradentate ligands.

EXPERIMENTAL SECTION

All the chemicals were purchased from commercial sources and used without purification. *Caution!!!* Although no problems were encountered in this work, silver perchlorate is potentially explosive. Only a small amount of the material was used and handled with great care. The ligands (**L1** and **L2**) were synthesized by adopting literature procedure.[29] NMR spectra (1D and 2D) of the ligands and their CPs were recorded on Bruker Avance DRX 400, and 500 NMR spectrometers and chemical shifts are expressed in ppm. Elemental analyses were performed on the Vario EL elemental analyzer. Mass spectra were measured with ABSciex QSTAR Elite ESI-Q-TOF mass spectrometer. Thermogravimetric (TG) analyses were performed under nitrogen with Perkin-Elmer STA 6000 analyzer. X-ray powder diffraction (**XRPD**) measurements were

performed on Panalytical X´Pert Pro MPD diffractometer operating at Cu Kα wavelength (1.54184 Å), and scans were performed at room temperature in the 2θ range 5−50°. Photoluminescence spectra were measured using Varian Cary Eclipse Fluorescence Spectrophotometer. Solid samples were ground to powder and pressed into the thin layer between quartz glass plates.

Synthesis of $\{[Ag(L1)]ClO_4\}_n$ (1)

A clear solution of $AgClO_4$ (41.5mg, 0.2 mmol) in acetonitrile (2 mL) was carefully layered on the top of ligand solution (L1; 63.3 mg, 0.2 mmol) in acetonitrile (3 mL). By next day, only a few crystals (2D-CP **1**) were obtained along with white precipitate. Recrystallization of white precipitate from a mixture of water and MeCN (2:8 v/v) gave colorless crystals of 2D-CP **1**.

$\{[Ag(L1)]ClO_4\}_n$ (**1**): Yield: 74.5 mg (≈71 %): ^{1}H NMR (400 MHz, DMSO-d_6) δ 8.43 (d, 2H), 8.27 (s, 2H), 7.52 (d, 2H), 7.47 (s, 2H), 7.31 (ddd, 2H), 7.11 (s, 2H), 5.75 (s, 4H). ^{13}C NMR (100 MHz, DMSO-d_6) δ 149.06, 148.59, 137.19, 135.43, 133.78, 128.35, 123.86, 122.74, 47.55. ^{1}H-^{15}N COSY NMR (DMSO-d_6 at 30 °C) δ= −207.39 (N1; imidazole), −118.71 (N2; imidazole) and −70.47 (N3; pyridine). ESI-Q-TOF-MS Calcd for $[Ag(L1)]^+$ $(C_{18}H_{16}N_6Ag)^+$: 423.0482; found: 423.0475. Anal. Calcd for $C_{18}H_{16}N_6\ ClO_4Ag$: C, 41.28: H, 3.08; N, 16.5. Found: C, 41.33; H, 3.17; N, 16.46.

Synthesis of $\{[Ag(L2)_{1.5}]ClO_4\cdot C_2H_3N\}_n$ (2a) and $\{[Ag(L2)]ClO_4\}_n$ (2b)

A clear solution of $AgClO_4$ (41.5mg, 0.2 mmol) in acetonitrile (2 mL) was carefully layered on the top of ligand solution (L2; 63.3 mg, 0.2 mmol) in acetonitrile (3 mL). By next day, a single crystal of 2D-CP **2a** was found in a test tube along with white precipitate. When the product was

redissolved in a mixture of water and MeCN (2:8 v/v), the colorless crystals of 1D-CP **2b** were formed.

Or

A clear solution of $AgClO_4$ (20.7 mg, 0.1 mmol) in water (0.4 mL) was added to the ligand solution (L2; 32 mg, 0.1 mmol) in acetonitrile (1.6 mL). In a week of period, colorless crystals of **2b** were obtained in a solution.

$\{[Ag(L2)]ClO_4\}_n$ (**2b**): Yield: 38.5 mg (≈74 %): ^{1}H NMR (400 MHz, DMSO-d_6) δ 8.43 (d, 4H), 7.42 (d, 2H), 7.10 (d, 2H), 6.95 (d, 4H), 5.82 (s, 4H). ^{13}C NMR (100 MHz, DMSO-d_6) δ 149.93, 147.37, 137.38, 128.26, 123.00, 121.74, 49.00. ^{1}H-^{15}N COSY NMR (DMSO-d_6 at 30 °C) δ −212.88 (N1; imidazole), −119.39 (N2; imidazole) and −73.54 (N3; pyridine). ESI-Q-TOF-MS Calcd for $[Ag(L2)]^+$ $(C_{18}H_{16}N_6Ag)^+$: 423.0482; found: 423.049. Anal. Calcd for $C_{18}H_{16}N_6ClO_4Ag$: C, 41.28: H, 3.08; N, 16.5. Found: C, 41.32; H, 3.24; N,16.39.

Synthetic procedure for zinc CPs (3 & 4)

A clear solution of $ZnCl_2$ (27.3 mg, 0.2 mmol) in methanol (3 mL) was carefully layered on the top of ligand solution (63.3 mg, 0.2 mmol) in chloroform (2 mL). By next day, only few colorless crystals were obtained in test tube for CP **4** along with white precipitate and only precipitate was obtained for CP **3**. Single crystals of CPs **3** and **4** were also obtained by dissolving the precipitate into the mixture of water and DMSO (1:9 v/v).

$[Zn(L1)Cl_2]_n$ (**3**): Yield: 81 mg (89.4 %): ^{1}H NMR (400 MHz, DMSO-d_6) δ 8.43 (dd, 2H), 8.40 (d, 2H), 7.48 (dt, 2H), 7.44 (d, 2H), 7.27 (ddd, 2H), 7.10 (d, 2H), 5.77 (s, 4H). ^{13}C NMR (100 MHz, DMSO-d_6) δ 148.58, 148.50, 137.27, 135.18, 133.74, 128.19, 123.73, 122.60, 47.46. ^{1}H-

^{15}N COSY NMR (DMSO-d_6 at 30 °C) δ −207.60 (N1; imidazole), −118.42 (N2; imidazole) and −62.15 (N3; pyridine). ESI-Q-TOF-MS Calcd for $[Zn(L1)Cl]^+$ $(C_{18}H_{16}N_6ZnCl)^+$: 415.0411; found: 415.0473. Anal. Calcd for $C_{18}H_{16}N_6Cl_2Zn$: C, 47.76: H, 3.56; N, 18.57. Found: C, 47.61; H, 3.73; N, 18.49.

$\{[Zn(L2)Cl_2]\cdot CHCl_3\}_n$ (4): Yield: 82.6 mg (91.2 %): ^{1}H NMR (400 MHz, DMSO-d_6) δ 8.43 (dd, 4H), 7.40 (d, 2H), 7.07 (d, 2H), 6.98 (d, 4H), 5.84 (s, 4H). ^{13}C NMR (100 MHz, DMSO-d_6) δ 149.52, 147.70, 137.41, 128.20, 122.95, 121.81, 49.04. ESI-Q-TOF-MS Calcd for $[Zn(L2)Cl]^+$ $(C_{18}H_{16}N_6ZnCl)^+$: 415.0411; found: 415.0392. Anal. Calcd for $C_{18}H_{16}N_6Cl_2Zn$: C, 47.76: H, 3.56; N, 18.57. Found: C, 47.70; H, 3.68; N, 18.52.

Synthesis of $\{[Cu(L1)_2Cl]Cl\cdot H_2O\}_n$ (5)

A solution of $CuCl_2.2H_2O$ (34.1 mg, 0.2 mmol) in methanol (2 mL) was carefully layered on top of ligand solution (L1; 126.6 mg, 0.4 mmol) in methanol (3 mL). The reaction only leads us to blue-colored precipitate. The mixture was stirred for *ca.* 30 min at room temperature to ensure the completion of the reaction. The precipitate was filtered and washed with methanol and dried under vacuum. Single crystals of **5** were obtained from DMSO at room temperature.

Yield: 120 mg (78.2 %): ESI-Q-TOF-MS Calcd for $[Cu(L1)_2Cl]^+$ $(C_{36}H_{32}N_{12}CuCl)^+$: 730.1852; found: 730.1845. Anal. Calcd for $C_{36}H_{32}N_{12}Cl_2Cu.H_2O$: C, 55.07: H, 4.36; N, 21.41. Found: C, 54.91; H, 4.42; N, 21.38.

Synthesis of $[Cu_2(L2)_2(\mu\text{-}Cl)_2]_n$ (6)

A water solution (0.2 mL) of $CuCl_2.2H_2O$ (34.1 mg, 0.2 mmol) was added to the DMSO solution (0.8 mL) of **L2** (63.3 mg, 0.2 mmol) and the resulting mixture was gently heated to obtain a clear

solution. During heating, the color of the solution turned from green to yellow. When the solution was cooled down to the room temperature, the pale yellow crystalline product was obtained. The product was washed several times with water and dried under vacuum. Yield: 43.5 mg (52.3 %): Anal. Calcd for $C_{18}H_{16}N_6ClCu$: C, 52.05: H, 3.88; N, 20.23. Found: C, 51.88; H, 4.08; N, 20.12. ESI-Q-TOF-MS Calcd for $[Cu(L2)]^+$ $(C_{18}H_{16}N_6Cu)^+$: 379.0732; found: 379.0727.

Formation of $[Cu_4(L2)_2(\mu\text{-}Cl)_4]_n$ (7): Only a few single crystal of **7** was found along with **6** as a byproduct in the synthesis of **6** described above. To improve the yield of **7**, the molar ratio of metal to ligand (**L2**) was changed from 1:1 to 2:1. However, even in these reaction conditions the compound **6** was the dominating product, and the compound **7** remained as a minor side product.

X-ray Data Collection

The single crystals of ligands (**L1** and **L2**) and their CPs were immersed in cryo-oil, mounted in a MiTeGen loop and measured at 120–123 K. The X-ray diffraction data were collected on Agilent Technologies Supernova diffractometer using Mo $K\alpha$ (λ = 0.71073 Å) or Cu Kα (λ = 1.54184 Å) radiation. The *CrysAlisPro*[41] program packages were used for cell refinements and data reductions. Structures were solved by either charge-flipping method using a *SUPERFLIP*[42] program or by direct methods using *SHELXS–2008*[43] or *SHELXT–2015*[43] programs. Gaussian or Multi-scan absorption correction was applied to all data, and structural refinements were carried out using *SHELXL–2015*[43] software. Details of data collections and structure refinements for CPs **1-7** are given in Table 1, while those of ligands (**L1** and **L2**) and **4a** are given in Table S2. In CP **7**, solvent molecules could not be unambiguously determined, and therefore the contribution of the missing solvent to the calculated structure factor was taken into account by using the SQUEEZE routine of PLATON.

RESULTS AND DISCUSSION

All the CPs of Cu(I), Cu(II), Zn(II), and Ag(I) with ligands **L1** and **L2** were synthesized *via* self-assembly.[44] The structures of coordination polymers in the solid state were determined by using single crystal X-ray diffraction, and their photoluminescence properties were screened using solid-state photoluminescence spectroscopy. Bulk phase purity of all the CPs (**1, 2b–6**) were confirmed by powder X-ray diffraction. The diffractograms are given in the supporting information (Figure S19−S21). In all cases, the experimental patterns matched well with the simulated patterns based on the single-crystal X-Ray diffraction results. The *N*-coordination of the ligand in Ag and Zn based CPs was also investigated in solution (DMSO-d_6) by 1D (^{1}H & ^{13}C) and 2D (^{1}H-^{15}N) NMR spectroscopy. Structures in the gas phase were analyzed by mass spectrometry (ESI-MS).

Silver(I) CPs from L1 (1; {[Ag(L1)]ClO_4}$_n$) and L2 (2a; {[Ag(L2)$_{1.5}$]ClO_4·C_2H_3N}$_n$ & 2b; {[Ag(L2)]ClO_4}$_n$)

The reaction of $AgClO_4$ with **L1** and **L2** at 1:1 molar amounts gave two-dimensional coordination polymers (2D-CPs; **1** & **2a**) and one-dimensional coordination polymer (1D-CP; **2b**) respectively. Single crystals of 2D-CPs with the ligand **L1** (**1**) and **L2** (**2a**) were obtained from slow diffusion of metal solution into the ligand solution in acetonitrile. The product **2b** was obtained as an inseparable mixture with **2a**. However, when the synthesis was carried out in a mixture of water and MeCN (2:8 v/v), **2b** could be obtained as a pure product with no **2a**. The 2D-CPs were crystallized in triclinic space group $P\ \bar{1}$, while the 1D-CP was crystallized in orthorhombic space group $P2_12_12$.

In **1** (Figure 2), all the nitrogen atoms ($2N_{Im}$ and $2N_{Py}$) from **L1** were involved in coordination with four different silver atoms. The asymmetric unit contains one full ligand molecule and a silver atom along with the perchlorate anion. The coordination geometry around the silver is distorted tetrahedron with the N4Ag binding set.[45,46] The imidazole rings of biim are twisted out of plane (68.72°) due to bridging coordination of biim. Each silver atom is coordinated by two pyridine nitrogen atoms [$Ag{-}N_{Py}$ = 2.268(6) Å & 2.372(6) Å] and two imidazole nitrogen atoms [$Ag{-}N_{Im}$ = 2.293(6) Å & 2.385(6) Å] from four different ligand molecules to generate 2D layered structure (Figure S3). These 2D layers are packed as parallel layers, which interact with each other *via* several weak $C{=}C{-}H_{Py}\cdots O$ and $CH_2\cdots O$ hydrogen bonds through the perchlorate anion (Table S1). The $Ag{-}N_{Py}$ and $Ag{-}N_{Im}$ bond distances are in good agreement with those reported for silver complexes with imidazole and pyridine derivatives.[45-48]

In solution, the ^1H NMR spectrum of **1** showed a minimal downfield shift for imidazole proton (H2, 0.07 ppm) as well as a upfield shift for pyridine hydrogen (H5, 0.17 ppm) atom compared to that of free ligand **L1**. In addition to ^1H NMR, we also recorded ^1H-^{15}N COSY spectra for **L1** and CP **1** (Figure S12b). A significant upfield shift was observed for N_{Py} (8.46 ppm) and N_{Im} atoms (2.15 ppm) compared to the free ligand, which is an indication of pyridine and biimidazole coordination. These changes in the chemical shifts support the observed solid-state structure where silver ions are coordinated by the N_{Im} and N_{Py} atoms from the ligand.

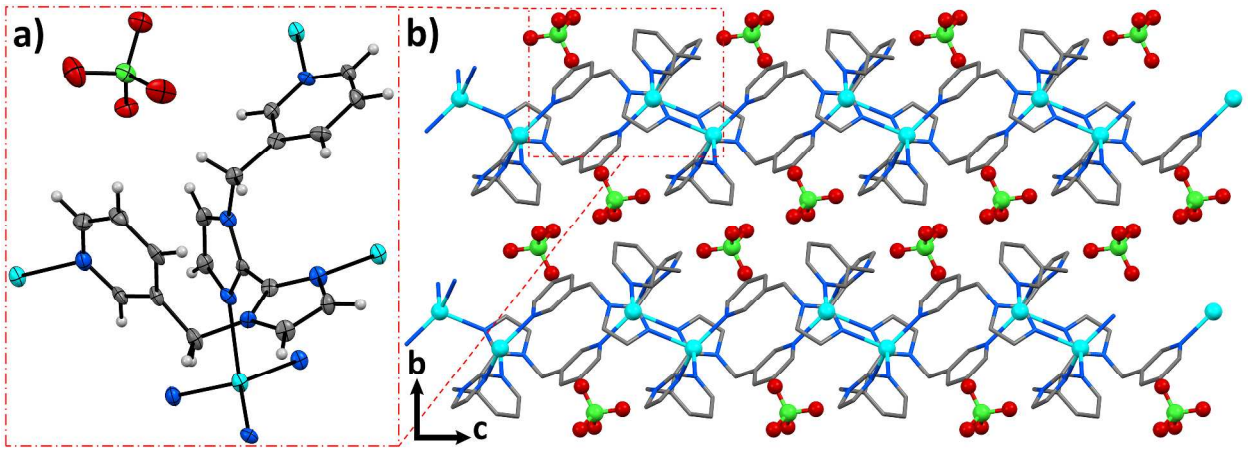

Figure 2. ORTEP plot (50% probability level) of **L1** coordination environment in silver CP **1** (a) and of the crystal packing of **1** viewed along the crystallographic *a*-axis (b).

The asymmetric unit of **2a** contains one complete ligand molecule, half a ligand molecule and a silver atom (2:3 of Ag to **L2**) along with perchlorate anion and acetonitrile solvent molecule. In **2a**, ligand **L2** exhibits two kinds of coordination modes: one is a μ_3-bridging mode with two N_{Im} and one N_{Py} atoms (uncoordinated pyridine ring shown in the red circle in Figure 3), and the other is a μ_2-bridging mode only with two N_{Py} atoms (uncoordinated biim ring shown in the purple box in Figure 3). The coordination geometry around the silver atom is again distorted tetrahedron with a N4Ag binding set. Similar to **1**, each silver atom is coordinated by two pyridine nitrogen atoms [Ag−N_{Py} = 2.316(7) Å & 2.512(8) Å] and two imidazole nitrogen atoms [Ag−N_{Im} = 2.267(7) Å & 2.277(8) Å] from four separate ligand molecules. In **1**, the crystal packing does not favor direct Ag···Ag contacts but in **2a** the shortest Ag···Ag distance (3.0898(1) Å) was found which might be an indication of the presence of argentophilic interactions and comparable with those observed in Ag (I) biim compounds.[47,48]

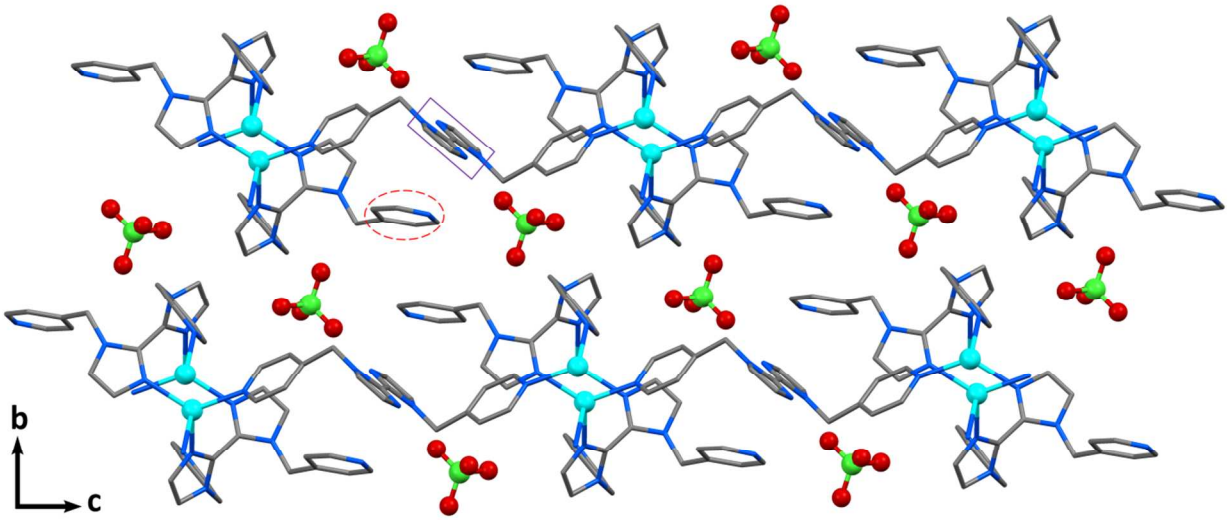

Figure 3. Crystal packing of **2a** viewed along the crystallographic *a*-axis. The uncoordinated pyridine ring is highlighted with a dotted circle and uncoordinate bridging biim with a solid box. Hydrogen atoms and solvent molecules (MeCN) are omitted for clarity.

The asymmetric unit of **2b** (Figure 4) contains two independent 1D polymeric chains where two ligand molecules are coordinated to two separate silver atoms (1:1 of Ag to **L2**), one full and two halves of perchlorate anions. In this case, the coordination geometry around the silver is almost linear[49] (N–Ag–N = 170.12(2)° & 171.18(2)°) and bridging coordination was observed from ligand molecule only through its pyridine nitrogen atoms [Ag–N_{Py} = 2.154(3) Å & 2.157(3) Å]. The two imidazole nitrogen atoms are not coordinated and the two imidazole rings are somewhat twisted out of the plane (the angle between the mean planes of the two imidazole rings is 28.89°). The shortest Ag···Ag distance between Ag atoms in adjacent chains is 3.690(4) Å & 3.725(6) Å. This value is longer than the sum of the van der Waals radii of two Ag atoms (3.44 Å), indicating that absence of argentophilic interactions. These 1D zigzag polymeric chains interact further with each other through perchlorate anions *via* several weak C=C–H_{Py}···O, C=C–H_{Im}···O and CH_2···O hydrogen bonds. (Table S1). In solution, the 1D-NMR (^{1}H & ^{13}C) spectral

results give no clear evidence on metal coordination, but in ^{1}H-^{15}N COSY spectra, only N_{Py} coordination was seen (5.51 ppm upfield shift for N_{Py}; Figure S13), which can be seen as evidence of CP **2b**.

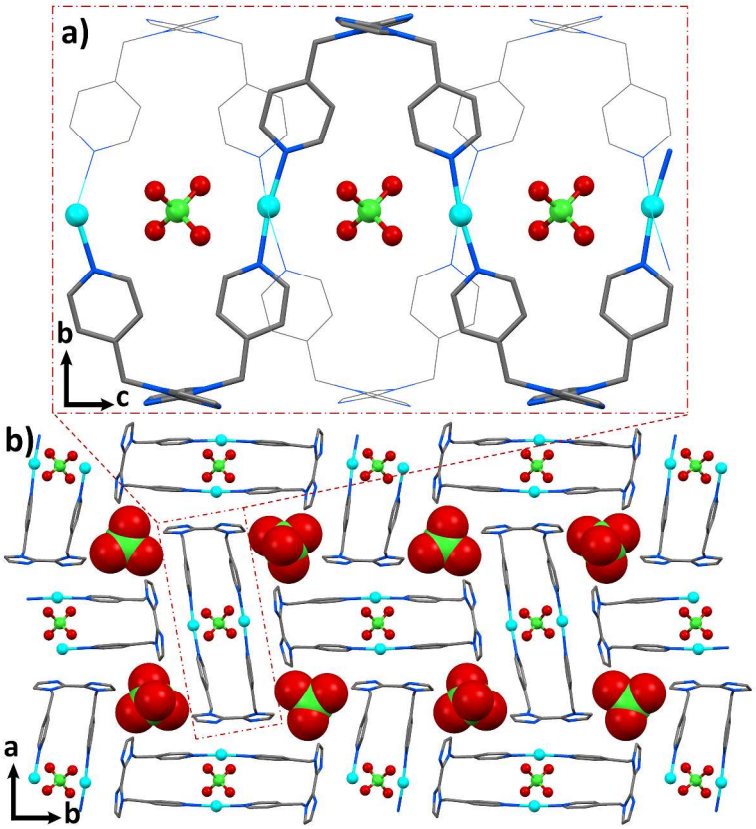

Figure 4. Top: one-dimensional chains of **2b** viewed along the crystallographic *a*-axis. Bottom: packing of the chains of **2b** viewed along the crystallographic *c*-axis. Hydrogen atoms are omitted for clarity.

Structures of Zinc (II) CPs from L1 $[Zn(L1)Cl_2]_n$ (3) and L2 $\{[Zn(L2)Cl_2]\cdot CHCl_3\}_n$ (4)

Two 1D-CPs (**3** and **4**) were obtained from the reaction of $ZnCl_2$ with **L1** or **L2** respectively. The single crystals of **3** (Figure 5a,b) were obtained from a mixture of water and DMSO (2:8 v/v) and

4 either from careful diffusion of metal solution (MeOH) into the ligand solution in chloroform (Figure 5c,d) or simply by dissolving obtained CP into the mixture of water and DMSO (2:8 v/v; Fig. **S5**; **4a**).

Both CPs, **3** and **4** were crystallized in the monoclinic $P2_1/c$ space group. Solid state structures of **3** and **4** revealed that the coordination geometry around the metal was in both cases slightly distorted tetrahedron. Furthermore, both the ligands **L1** and **L2** acted as bidentate bridging ligands. In **3**, only imidazole nitrogen atoms [Zn−N_{Im} = 2.031(2) Å & 2.032(2) Å] are involved in coordination, and the Zn–N_{Im} distances are close to those found in molecules such as $[Zn(Me_2biim)Cl_2]_n$.[27] In **4** only pyridine nitrogen atoms are involved in coordination while imidazole rings remained free of coordination. The Zn–N_{Py} (2.044(2) Å & 2.047(2) Å) distances in **4** are in very good agreement with those found in molecular structures such as $[Zn(4,4'\text{-bipy})Cl_2]_n$.[50] The coordination spheres in **3** and **4** are completed with two chlorido ligands [Zn−Cl1 = 2.223(5) Å, Zn−Cl2 = 2.244(5) Å in **3**; Zn−Cl1 = 2.217(7) Å, Zn−Cl2 = 2.239(7) Å in **4**] leading to 1D-zigzag infinite chains. Due to imidazole coordination in **3**, two imidazole rings are twisted out of plane (the angle between the mean planes of the two imidazole rings is 64.38°). However, in **4** the imidazole rings are completely coplanar. In **4**, the solvent molecule ($CHCl_3$) was trapped in the crystal packing by forming weak Cl_3C−H···N_{Im} hydrogen bonding (Table S1). In crystal packing of **4**, the adjacent 1D chains interact each other *via* several weak C=C–H_{Im}···Cl and CH_2···Cl hydrogen bonds to the chlorido ligand (Cl^-). In **3**, several weak intra and intermolecular hydrogen bonds were observed between the chlorido ligand and aromatic or aliphatic hydrogen atoms and also C=C–H_{Py}···N_{Py}.

In solution, both 1D and 2D NMR (Figure S12c) spectra indicate N_{Im} coordination to the zinc atom in CP **3.** A minimum downfield shift for imidazole proton (H2, 0.03 ppm) was seen in ^{1}H

NMR spectrum, and it is also supported with ^{1}H-^{15}N COSY spectra (N_{Im}, 1.18 ppm upfield shift). The ^{1}H NMR spectra of CP **4** indicate N_{Py} coordination (0.04 ppm downfield from H4) to the zinc atom.

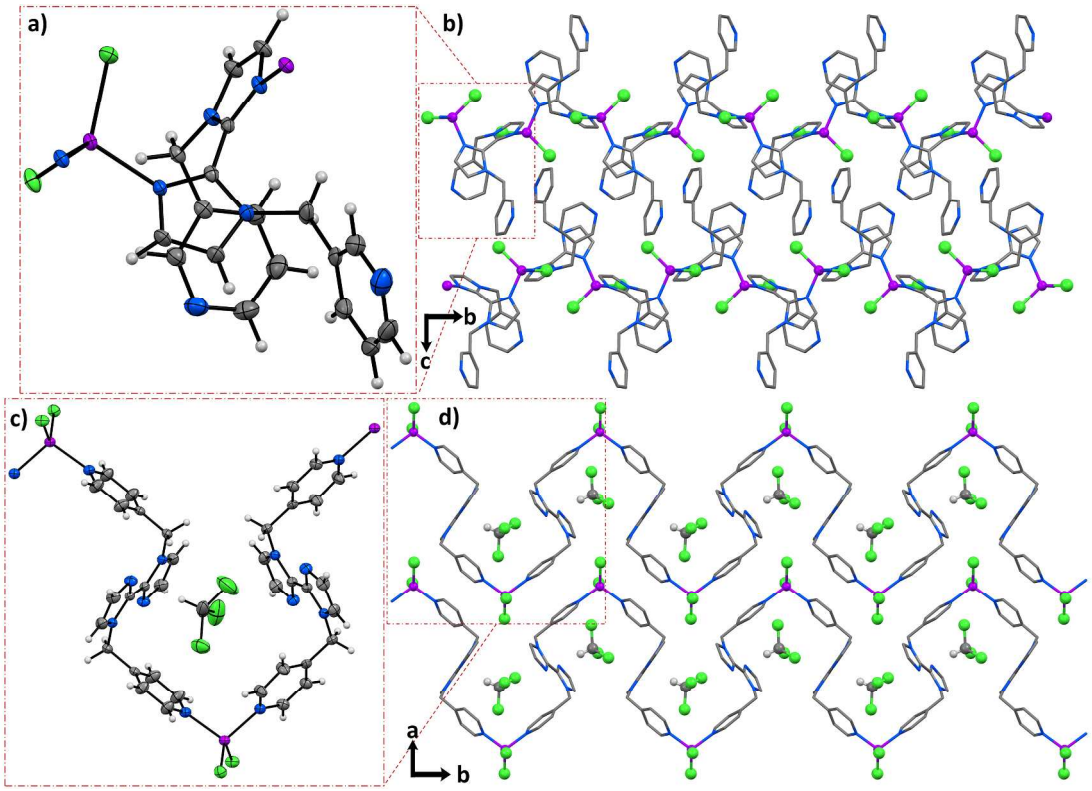

Figure 5. ORTEP plot (50% probability level) of ligand coordination environment in zinc CPs with **L1** (**3**, a) and **L2** (**4**, c). Crystal packing of **3** (b) and **4** (d) along the crystallographic *a*-axis and *c*-axis, respectively. Hydrogen atoms are omitted for clarity.

Structures of $\{[Cu(L1)_2Cl]Cl\cdot H_2O\}_n$ (5) from L1

The reaction of $CuCl_2\cdot 2H_2O$ with ligand **L1** in 1:1 ratio gave unexpectedly crystals of the two-dimensional CP **5,** where **L1** was acting as a bidentate bridging ligand and was coordinated only through its N_{Py} atoms (Figure 6). The yield of CP **5** was improved by changing the molar ratio of metal to ligand from 1:1 to 1:2. Single crystals of **5**, crystallized in tetragonal space group

*P*4/ncc, were obtained from DMSO. The asymmetric unit contains half a ligand molecule, Cu^{2+} ion, chlorido ligand, and a chloride anion along with a disordered water molecule. The coordination geometry around the copper atom is square pyramidal with a N4ClCu binding set.[51,52] Each copper atom is coordinated by four pyridine nitrogen [Cu−N_{Py} = 2.041(2) Å, Cu−Cl = 2.539(1) Å] atoms from four individual ligand molecules and imidazole nitrogens are free of coordination.

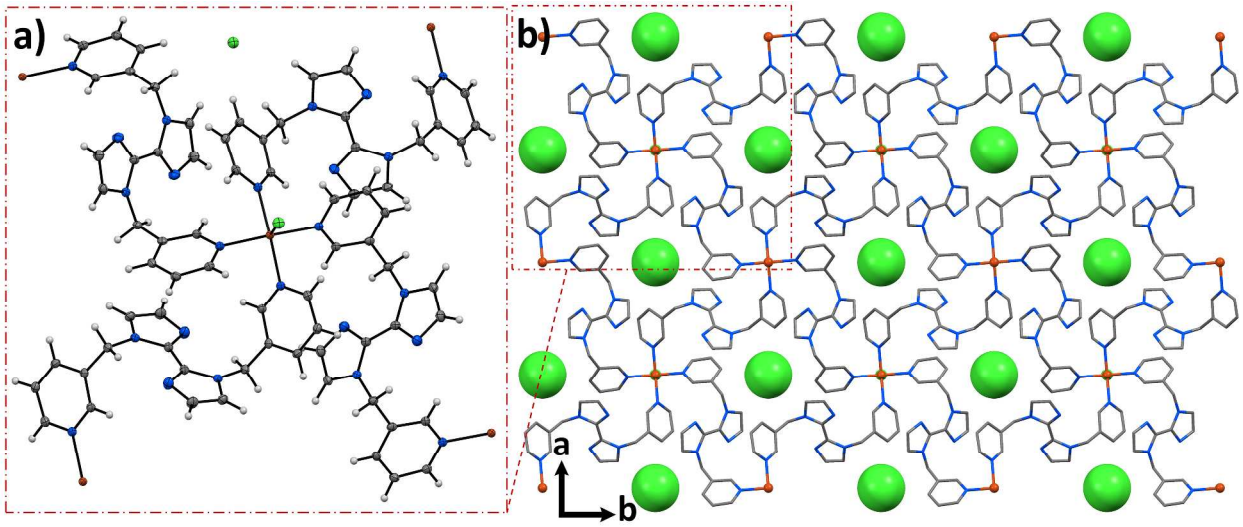

Figure 6. a) ORTEP plot (50% probability level) of coordination environment of Cu^{2+} in CP **5** with **L1.** (b) View of the 2D layered structure of **5** along the crystallographic *c*-axis. Solvent molecules (H_2O) and hydrogen atoms are omitted for clarity.

Structure of $[Cu_2(L2)(\mu\text{-}Cl)_2]_n$ (6) from L2

The reaction of $CuCl_2{\cdot}2H_2O$ with **L2** from a mixture of water and DMSO (2:8 v/v) at equimolar amounts gave 1D-CP **6** (Figure 7). In these reaction conditions, the copper was reduced from

Cu^{2+} to Cu^{+} and crystallized in monoclinic with $P2_1/c$ space group. Reduction of Cu(II) to Cu(I) in DMSO/Water solution is unusual, but under similar condition reduction of silver and gold have been reported. [53,54] The reduction of copper is also evident based on ESI-MS spectra, in which ion $[Cu(L2)]^{+}$ was observed. The asymmetric unit contains one full ligand molecule, Cu^{+} ion and one chlorido ligand (Cl adopts in μ_2-bridging mode). The coordination geometry around copper atom is distorted tetrahedron with two N_{Py} atoms [Cu−N_{Py} = 1.984(4) Å & 1.988(4) Å] from two different ligand molecules and two bridging chlorido ligands [Cu−Cl1= 2.511(7) Å, Cu−Cl1$^{\#1}$= 2.502(5) Å ($^{\#1}$= −X, 2−Y, 1−Z)] and Cu···Cu distance is 2.849(1) Å. The distortion from ideal tetrahedral geometry arises from the angle of N−Cu−N (149.74°). The two N_{Im} atoms are not coordinated, and the two imidazole rings are twisted out of plane (the angle between the mean planes of the two imidazole rings is 31.56°). The copper atoms and bridging chlorido ligands are positioned on the same plane, with no deviation from planarity, which is caused by a symmetry operation, resulting in a Cl−Cl separation of 4.126(2) Å. These 1D chains interact with each other *via* weak C=C−H_{Im}···N_{Im} and CH_2···N_{Im} hydrogen bonding interactions.

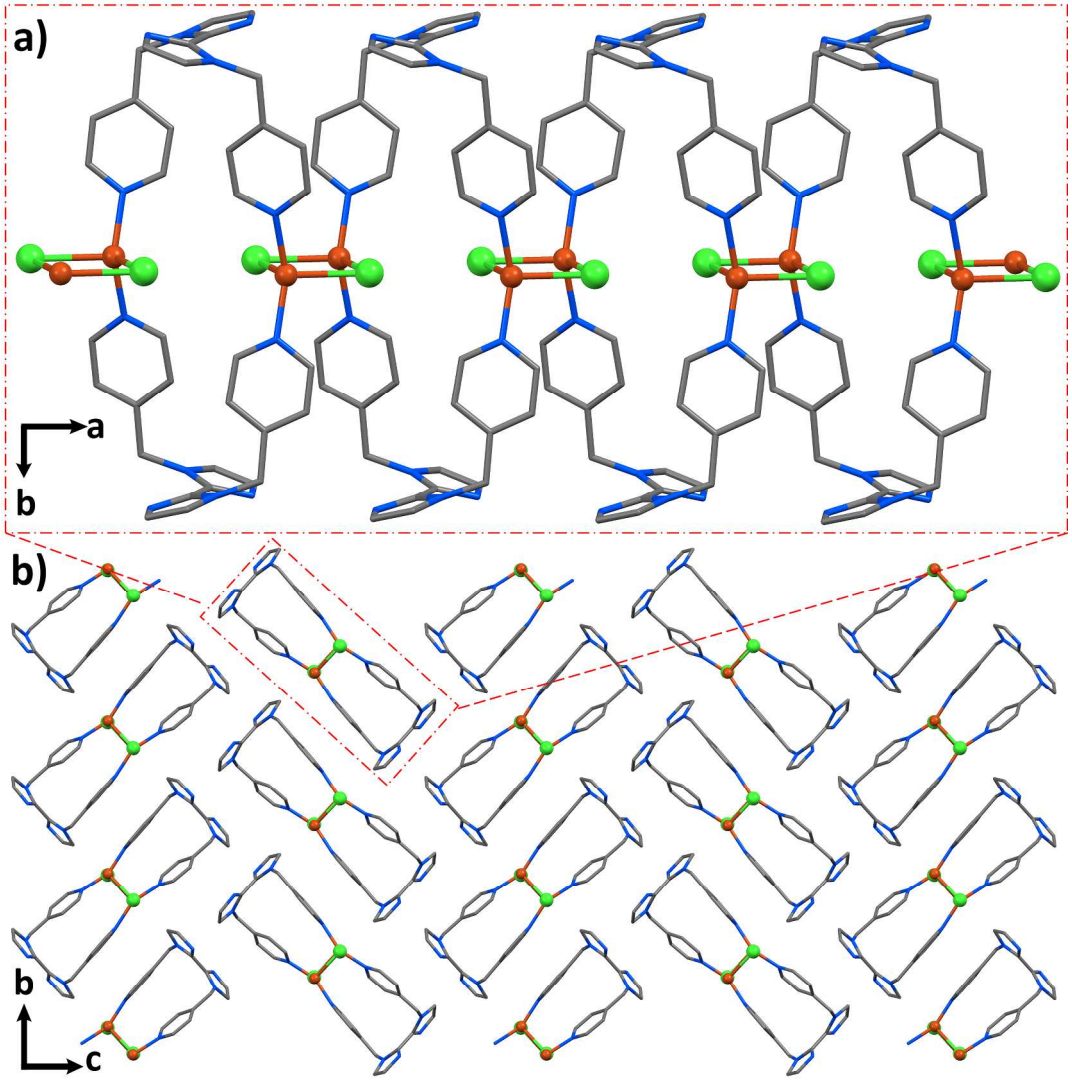

Figure 7. Top: one-dimensional chains of **6** viewed along the crystallographic *c*-axis. Bottom: packing of the chains of **6** viewed along the crystallographic *a*-axis.

Crystal structure of $[Cu_4(L2)(\mu\text{-}Cl)_4]_n$ (7) from L2

Upon X-ray diffraction, it was revealed that in **7** (Figure 8) the copper was reduced to Cu^+ as in CP **6**. Despite several attempts, no rational route to pure **7** without **6** could be developed. The CP **7** was crystallized in trigonal space group $R\ \bar{3}c$. The asymmetric unit contains half of the ligand

molecule, Cu^{+} ion, and chlorido ligand. The geometry around the copper atom is again distorted tetrahedron with one N_{Py} atom [$Cu-N_{Py}$ = 2.025(4) Å] and one N_{Im} atom [$Cu-N_{Im}$ = 1.981(4) Å] from two separate ligand molecules. The coordination sphere is completed by two bridging chlorido ligands [Cu−Cl = 2.421(2) Å, $Cu-Cl^{\#1}$ = 2.411(1) Å]. The Cu···Cu distance is 2.696(1) Å which is shorter than the sum of van der Waals radii (2.8 Å) and an indication of the presence of cuprophilic interactions.[55]

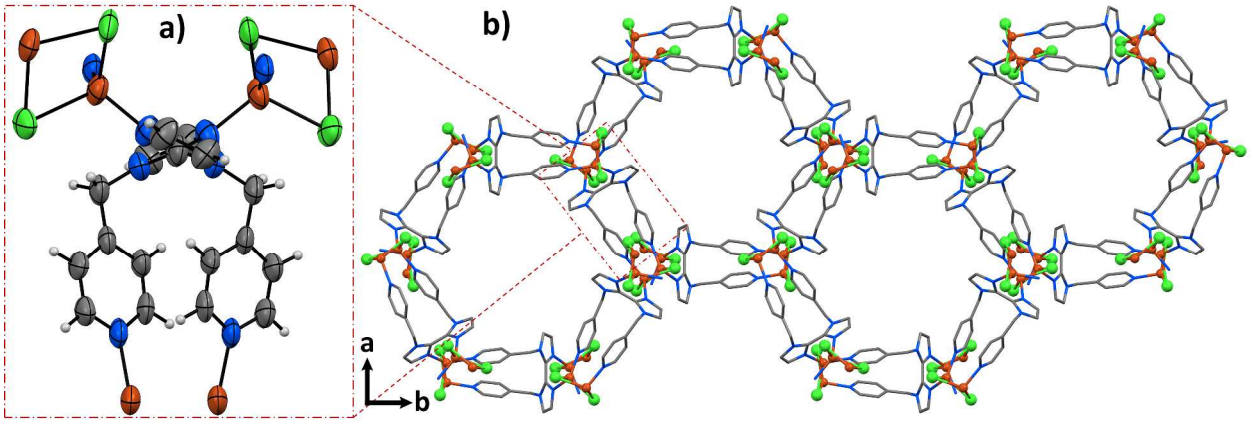

Figure 8. a) ORTEP plot (50% probability level) of **L2** coordination environment in Cu^{+} CP **7.** (b) Crystal packing of **7** viewed along the crystallographic *c*-axis.

Table 1. Crystallographic data for CPs **1–7**

	1	**2a**	**2b**	**3**	**4**	**5**	**6**	**7**
Formula	$C_{18}H_{16}N_6Ag$, ClO_4	$C_{27}H_{24}N_9Ag$, ClO_4, C_2H_3N	$2(C_{18}H_{16}N_6Ag)$, $2(ClO_4)$	$C_{18}H_{16}N_6Cl_2Zn$	$C_{18}H_{16}N_6Cl_2$ Zn, $CHCl_3$	$C_{36}H_{32}N_{12}ClCu$, H_2O	$C_{18}H_{16}N_6Cl$ Cu	$C_9H_8N_3ClCu$
fw	523.69	722.92	1047.37	452.64	572.01	785.19	415.36	257.17
Temp (K)	120	120	120	120	120	120	123	123
Cryst Syst	Triclinic	Triclinic	Orthorhombic	Monoclinic	Monoclinic	Tetragonal	Monoclinic	Trigonal
Space group	$P\ \bar{1}$	$P\ \bar{1}$	$P2_12_12$	$P2_1/c$	$P2_1/c$	$P4/ncc$	$P2_1/c$	$R\ \bar{3}c$
a (Å)	9.574(2)	9.714(7)	23.020(2)	8.982(4)	12.291(3)	16.499(6)	6.808(2)	27.849(2)
b (Å)	9.657 (1)	10.624(1)	22.779(2)	10.061(3)	13.905(3)	16.499(6)	9.658(2)	27.849(2)
c (Å)	10.870(2)	16.101(1)	7.0740(6)	24.625(1)	14.808(4)	12.266(9)	27.070(9)	22.093(8)
α (°)	91.746(1)	71.458(9)	90.00	90	90	90	90	90
β (°)	105.911(1)	76.979(7)	90.00	122.878(7)	110.538(3)	90	105.397(3)	90
γ (°)	102.003(1)	75.869(8)	90.00	90	90	90	90	120
V ($Å^3$)	941.3(2)	1508.0(3)	3709.31(5)	1868.87(2)	2369.93(1)	3339.0(3)	1716.07(9)	14839.0(2)
d_{calc} (g/cm^3)	1.848	1.592	1.876	1.609	1.603	1.562	1.608	1.036
Z	2	2	4	4	4	4	4	36
μ (mm^{-1})	1.254	0.811	10.422	1.616	1.620	2.826	3.351	1.036
Ref.Collected	5616	9875	23418	29060	15572	8434	12080	9855
Ind. Ref	3397	5267	7669	4291	4654	1728	3522	3150
R_{int}	0.0592	0.0696	0.0281	0.0455	0.0276	0.0277	0.0497	0.0461
F (000)	524	734	2096	920	1152	1620	848	4644
GOF	1.162	1.045	1.021	1.060	1.034	1.081	1.168	4644
R1[a] ($I \geq 2\sigma$)	0.0728	0.0809	0.0267	0.0302	0.0378	0.0388	0.0616	0.0614
wR2b($I \geq 2\sigma$)	0.1280	0.3004	0.0681	0.0695	0.0977	0.1122	0.1640	0.1820

Thermal Analysis

To evaluate the thermal stability of CPs **1, 2b–6**, their thermal decomposition behaviors were studied by TGA (Figure 9). The experiments were performed under nitrogen atmosphere at a heating rate of 10 °C min^{-1} in the temperature range of 30−700 °C. The TGA curves of silver CPs (**1, 2b**) showed that their networks were stable up to 288 and 283 °C, respectively. Beyond these temperatures, the networks began to decompose. The TGA curve of **3** showed that the network was stable up to 393 °C and then started to decompose on further heating. For CPs **4** and **5**, the first weight losses between 50−350 and 50−220 °C correspond to the loss of the solvent of crystallization, i.e. chloroform (expt. 20.97%; calcd. 20.87%) and water (expt. 1.93%; calcd. 2.01%) molecules, respectively. The CP network of **4** and **5** began to decompose beyond 405 °C and 247 °C, respectively. The CP network of **6** was found to be stable up to 260 °C and then started to decompose.

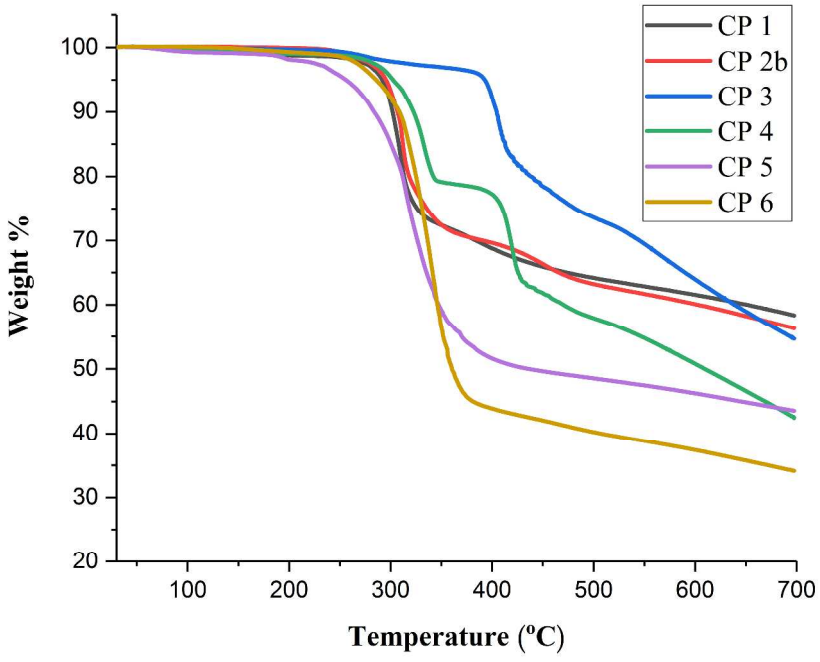

Figure 9. TGA curves of the CPs **1, 2b–6** recorded at a heating rate of 10 °C min^{-1}.

PHOTOLUMINESCENCE IN SOLID STATE

Photoluminescence properties of the obtained CPs **1**, **2b**, **3**–**6** and free ligands **L1** and **L2** in solid state were examined, and obtained spectra are presented in Figure10.

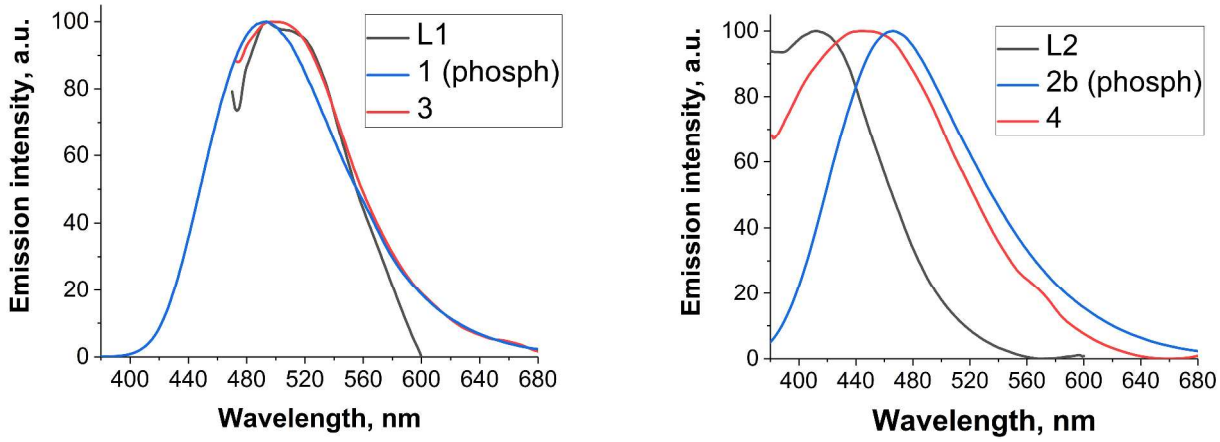

Figure 10. Normalized photoluminescence spectra of **L1** and its CPs **1** and **3** (left) and **L2** and its CPs **2b** and **4** (right).

The free ligands **L1** and **L2** display fluorescence with different emission maxima at 495 nm (excitation at 450 nm) for **L1** and 410 nm (excitation at 350 nm) for **L2**. It has to be pointed out that fluorescence emission of both **L1** and **L2** in the solid state depends on excitation wavelength and possesses additional emission peaks in UV range (see ESI for fluorescence excitation-emission matrices). Similar dual fluorescence can be seen in literature for biim[56] and its dimethyl derivatives[57] in the solid state. A detailed study of the nature of such luminescent properties of **L1** and **L2** requires a comprehensive analysis that is beyond of the scope of this work.

Silver-based CPs, **1** and **2b** do not display any detectable fluorescence but exhibit intense phosphorescence with emission maxima at 490 nm (excitation at 280 nm) for **1**, and at 465 nm (excitation 250 nm) for **2b**. The absence of fluorescence can be attributed to the heavy atom

effect of the metal center. The ability of silver(I) cation to promote inter-system crossing to the triply excited states within coordination polymers is well known in the literature.[58]

Zinc-based CPs, **3** and **4** both possess fluorescence emission with maxima at 495 nm (excitation at 450 nm) for **3** and 445 nm (excitation at 370 nm) for **4**. Apart from fluorescence, both compounds display weak phosphorescence emission at 520 nm.

Copper-based CPs (**5** and **6**), do not display any detectable fluorescence or phosphorescence. Quenching of luminescence is common in copper(II) (*via* electron or energy transfer)[59] and copper(I) (*via* excited state distortions)[60] containing compounds.

Unambiguous assignment of the observed photoluminescence band to a certain electronic transition without further spectroscopic and computational studies is challenging due to complicated fluorescence of **L1** and **L2** in the solid state. Nonetheless, some interesting observations can be nonetheless pointed out based on obtained data. As can be seen in Figure 10, CPs **1** and **3** display nearly same luminescence as the free ligand **L1**. As discussed above, in these CPs the metal atoms are coordinated to the biimidazole nitrogen atoms of **L1**, while pyridine nitrogen atoms remain free. On the other hand, only the pyridine atoms of **L2** ligand are coordinated in CPs **2b** and **4,** and therefore a significant shift of emission maximum compared to the free ligand can be observed. Therefore, luminescent properties of the obtained CPs are not only defined by nature of metal ion (whether luminescence will be quenched or not) but are also influenced by the mode of coordination of the ligand. This provides a potential tool for fine-tuning of emission wavelength and intensity *via* design of the ligand. Since the emission is within the visible range, CPs containing **L1** and **L2** ligands may be useful for practical applications, such as the production of organic light emitting devices.

CONCLUSIONS

In summary, we have utilized two semi-rigid biimidazole based ligands (**L1** and **L2**) as organic linkers for the construction of several CPs from Ag, Zn, and Cu metal ions. These ligands display pyridine (N_{Py}) and imidazole (N_{Im}) coordination groups which differ in their coordination ability (N_{Py} coordination ability is higher than the N_{Im}).[28-30] According to the structures of these eight CPs, we have found that the final structure can be influenced by the structure of the ligand, nature of the metal ion, the molar ratio of reactants, and the reaction solvent used. The single crystal X-ray analyses of these eight CPs reveal versatile coordination modes of ligands, including bidentate (**2a**, **2b**, **3–6**), tridentate (**2a**), and tetradentate (**1, 7**), which are responsible for different structural topologies. The influence of reaction solvent on coordination geometry of silver atom was observed in CPs **1** and **2**. A linear (**2b**) coordination was obtained in a mixture of water and MeCN and tetrahedral coordination (**1, 2a**) in MeCN. An unusual reduction of Cu^{2+} to Cu^{+} in a mixture of water and DMSO was observed during the synthesis and formation of CPs **6** and **7**. The photophysical behavior of CPs 1–4 in the solid state was found to be dependent primarily on the nature of the metal center, but it was also influenced by the coordination mode of the ligand. The results show that the semi-rigid ligands such as **L1** and **L2** can be used to produce a range of coordination polymers with different structural and photophysical properties. Both the structures and the properties can be adjusted by choice of the metal and by modifying the reaction conditions.

SUPPORTING INFORMATION

Ligand synthesis (**L1** & **L2**) and single crystal X-ray data, selected bond lengths and angles for CPs **1–4**, Solid state photoluminescence of ligands, 2D NMR spectra of ligands and CPs **1-4**.

Accurate mass spectral results for all the CPs (**1, 2b–6**), EPR of CP **5**, and the experimental XRPD patterns of CPs **1, 2b–6** compared with the simulated pattern.

CORRESPONDING AUTHOR

*E-mail: matti.o.haukka@jyu.fi

ACKNOWLEDGEMENTS

TR, MH, and EK kindly acknowledge the financial support from the Academy of Finland (Proj. nos. 295581, 284562 and 278743). EU COST action CM 1302 “Smart Inorganic Polymers” is also gratefully acknowledged.

REFERENCES

(1) Getman, R. B.; Bae, Y-S.; Wilmer, C. E.; Snurr, R. Q. *Chem. Rev.* **2012**, *112*, 703–723.

(2) Lv, X.; Li, L.; Sun, X.; Zhang, H.; Cai, J.; Wang, C.; Tang, S.; Zhao, X. *Chem. Asian J.* **2014**, *9*, 901–907.

(3) Noro, S-I.; Mizutani, J.; Hijikata, Y.; Matsuda, R.; Sato, H.; Kitagawa, S.; Sugimoto, K.; Inubushi, Y.; Kubo, K.; Nakamura, T. *Nat. Commun*. **2015**, *6*, 5851 DOI: 10.1038/ncomms6851.

(4) Zhao, M.; Tan, J.; Su, J.; Zhang, J.; Zhang, S.; Wu. J. Tian, Y. *Dyes Pigm.* **2016**, *130*, 216–225.

(5) Melnic, E.; Coropceanu, E. B.; Forni, A.; Cariati, E.; Kulikova, O. V.; Siminel, A. V.; Kravtsov, V. C.; Fonari, M. S. *Cryst. Growth Des.* **2016**, *16*, 6275–6285.

(6) Wen, T.; Zhang, D-X.; Ding, Q-R.; Zhang, H-B.; Zhang, J. *Inorg. Chem. Front.* **2014**, *1*, 389–392.

(7) Zhang, W.; Xiong, R-G. *Chem. Rev.* **2012**, *112*, 1163–1195.

(8) Jiang, X.; Liu, C-M.; Kou, H-Z. *Inorg. Chem.* **2016**, *55*, 5880–5885.

(9) Sun, R. W-Y.; Zhou, X-P.; Wang, J-H.; Li, D. *Chem. Commun.* **2014**, *50*, 2295–2297.

(10) Wen, T.; Zhang, D-X.; Zhang, J. *Inorg. Chem*. **2013**, *52*, 12–14.

(11) Givaja, G.; Amo-Ochoa, P.; Gomez-Garcia, C. J.; Zamore, F. *Chem. Soc. Rev.* **2012**, *41*, 115–147.

(12) Minaev. B.; Baryshnikov, G.; Agren, H. Phys. *Chem. Chem. Phys.* **2014**, *16*, 1719–1758.

(13) Uemura, K. *Inorg Chem Commun.* **2008**, *11*, 741–744.

(14) Nath, K.; Husain, A.; Dastidar, P. *Cryst. Growth Des.* **2015**, *15*, 4635–4645.

(15) Dong, Y-B.; Jiang, Y-Y.; Li, J.; Ma, J-P.; Liu, F-L.; Tang, B.; Huang, R. Q.; Batten, S. R. *J. Am. Chem. Soc.* **2007**, *129*, 4520–4521.

(16) Wang, X-M.; Chen, S.; Fan, R-Q.; Zhang, F-Q.; Yang, Y-L. *Dalton Trans.* **2015**, *44*, 8107–8125.

(17) Cui, J-W.; An, W-J.; Hecke, K-V.; Cui, G-H. *Dalton Trans.* **2016**, *45*, 17474–17484.

(18) Zheng, S-R.; Yang, Q-Y.; Yang, R.; Pan, M.; Cao, R.; Su, C-Y. *Cryst. Growth Des.* **2009**, *9*, 2341–2353.

(19) Guo, X.; Guo, H.; Zou, H.; Qi, Y.; Chen, R. *CrystEngComm.* **2013**, 9112–9120.

(20) Bu, X-H.; Chen, W.; Lu, S-L.; Zhang, R-H.; Liao, D-Z.; Bu, W-M.; Shionoya, M.; Brisse, F.; Ribas, J. *Angew. Chem. Int. Ed.* **2001**, *40*, 3201–3203.

(21) Chen, C-L.; Zhang, J-Y.; Su, C-Y. *Eur. J. Inorg. Chem.* **2007**, 2997–3010.

(22) Xiao, J-C.; Twamley, B.; Shreeve, J. M. *Org. Lett.* **2014**, *6*, 3845–3847.

(23) Laurila, E.; Tatikonda, R.; Oresmaa, L.; Hirva, P.; Haukka, M. *CrystEngComm.* **2012**, *14*, 8401–8408.

(24) Mardanya, S.; Karmakar, S.; Mondal, D.; Baitalik, S. *Inorg. Chem.* **2016**, *55*, 3475–3489.

(25) Rommel, S. A.; Sorsche, D.; Fleischmann, M.; Rau, S. *Chem. Eur. J.* **2017**, DOI: 10.1002/chem.201605782.

(26) Zhu, H-F.; Fan, J.; Okamura, T-A.; Sun, W-Y.; Ueyama, N. *Cryst. Growth Des.* **2005**, *5*, 289–294.

(27) Yang, L-N.; Zhi, Y-X.; Hei, J-H.; Li, J.; Zhang, F-X.; Gao, S-Y. *J. Coord. Chem.* **2011**, *64*, 2912–2922.

(28) CCDC **1541300** and **1541301** contain the supplementary crystallographic data for ligands **L1** and **L2** respectively.

(29) Aakeröy, C. B.; Wijethunga, T. K.; Desper, J. *J. Molecular Stru.* **2014**, *1072*, 20–27.

(30) Aakeröy, C. B.; Wijethunga, T. K.; Desper, J.; Moore, C. *J Chem Crystallogr.* **2015**, *45*, 267–276.

(31) Aakeröy, C. B.; Wijethunga, T. K.; Desper, J. *New J. Chem.,* 2015, **39**, 822–828.

(32) Fu, Y-M.; Zhao, Y-H.; Lan, Y-Q.; Shao, K-Z.; Qiu, Y-Q.; Hao, X-R.; Su, Z-M. *J. Solid State Chem.* **2008**, *181*, 2378–2385.

(33) Zang, H-Y.; Tan, K.; Guan, W.; Li, S-L.; Yang, G-S.; Shao, K-Z.; Yan, L-K.; Su, Z-M. *CrystEngComm*. **2010**, *12*, 3684–3690.

(34) Khlobystov, A. N.; Blake, A. J.; Champness, N. R.; Lemenovskii, D. A.; Majouga, A. G.; Zyk, N. V.; Schröder, M. *Coord. Chem. Rev.* **2001**, *222*, 155–192.

(35) Chen, C-J.; Liu, F-N.; Zhang, A-J.; Zhang, L-W.; Liu, X. *Acta Cryst.* **2009**, *E65*, m1674–m1675.

(36) Kandaiah, S.; Huebner, R.; Jansen, M. *Polyhedron*. **2012**, *48*, 68–71.

(37) Tzeng, B-C.; Banik, M.; Selvam, T.; Lee, G-H. *Cryst. Growth Des*. **2013**, *13*, 4245–4251.

(38) Pedireddi, V. R.; Shimpi, M. R.; Yakhmi, J. V. *Macromol. Symp.* **2006**, *241*, 83–87.

(39) Jayamani, A.; Sengottuvelan, N.; Kang, S. K.; Kim, Y. I. *Polyhedron.* **2015**, *98*, 203–216.

(40) Tatikonda, R.; Kalenius, E.; Haukka, M. *Inorg. Chim. Acta.* **2016**, *453*, 298–304.

(41) Agilent, *CrysAlisPro*, Agilent Technologies, Yarnton, England, **2013**.

(42) Palatinus, L.; Chapuis, G. *J. Appl. Cryst*. **2007**, *40*, 786–790.

(43) Sheldrick, G. M. *Acta Crystallogr.* **2008**, *A64*, 112–122; *Acta. Cryst.* **2015**, *A71*, 3–8; *Acta. Cryst.* **2015**, *C71*, 3–8.

(44) Robin, A. Y.; Fromm, K. M. *Coord. Chem. Rev*. **2006**, *250*, 2127–2157.

(45) Jiang, J-J.; Li, X-P.; Zhang, X-L.; Kang, B-S.; Su, C-Y. *CrystEngComm.* **2005**, *7*, 603–607.

(46) Noh, T. H.; Choi, Y. J.; Ryu, Y. K.; Lee, Y-A.; Jung, O-S. *CrystEngComm*. **2009**, *11*, 2371–2374.

(47) Sang, R-L.; Xu, L. *Eur. J. Inorg. Chem.* **2006**, 1260–1267.

(48) Laurila, E.; Oresmaa, L.; Kalenius, E.; Hirva, P.; Haukka, M. *Polyhedron*. **2013**, *52*, 1231–1238.

(49) Wang, L-S.; Zhanf, J-F.; Yang, S-P. *Acta Cryst*. **2004**, *E60*, m1484–m1486.

(50) Hu, C.; Englert, U. *Angew. Chem. Int. Ed.* **2005**, *44*, 2281–2283.

(51) Linfoot, C. L.; Richardson, P.; Hewat, T. E.; Moudam, O.; Forde, M. M.; Collins, A.; White, F.; Robertson, N. *Dalton Trans.* **2010**, *39*, 8945–8956.

(52) Petrovic, K.; Potocnak, I.; Raczova, K.; Cizmar, E.; Petrovic, M. *Transition Met. Chem*. **2015**, *40*, 541–553.

(53) Tatikonda. R.; Bertula, K.; Nonappa, N.; Hietala, S.; Rissanen, K.; Haukka, M. *Dalton Trans.* **2017**, *46*, 2793–2802.

(54) Nitsch, J.; Lacemon, F.; Lorbach, A.; Eichhorn, A.; Cisnetti, F.; Steffen, A. *Chem. Commun.* **2016**, *52*, 2932–2935.

(55) Nitsch, J.; Lacemon, F.; Lorbach, A.; Eichhorn, A.; Cisnetti, F.; Steffen, A. *Chem. Commun.* **2016**, *52*, 2932–2935.

(56) Shi, Z.; Peng, J.; Zhang, Z.; Yu, X.; Alimaje, K.; Wang, X. *Inorg. Chem. Commun.* **2013**, *33*, 105–108.

(57) Sang, R.; Xu, L. *Inorg. Chem.* **2005**, *44*, 3731–3737.

(58) Xiao, Y-H.; Huang, J.; Deng, Z-P.; Huo, L-H.; Gao, G. *J. Solid State Chem.* **2017**, *251*, 255-265.

(59) Chen, H-F.; Yang, W-B.; Lin, L.; Guo, X-G.; Dui, X-J.; Wu, X-Y.; Lu, C-Z.; Zhang, C-J. *J. Solid State Chem*. **2013**, *201*, 215–221.

(60) Eggleston, M. K.; Fanwick, P. E.; Pallenberg, A. J.; McMillin, D. R. *Inorg. Chem*. **1997**, *36*, 172-176.

Table of Contents Entry for:

Construction of coordination polymers from semi-rigid ditopic 2,2´-biimidazole derivatives: synthesis, crystal structures, and characterization

Rajendhraprasad Tatikonda, Evgeny Bulatov, Elina Kalenius and Matti Haukka*

Department of Chemistry, University of Jyväskylä, P. O. Box 35, FI-40014 Jyväskylä, Finland.

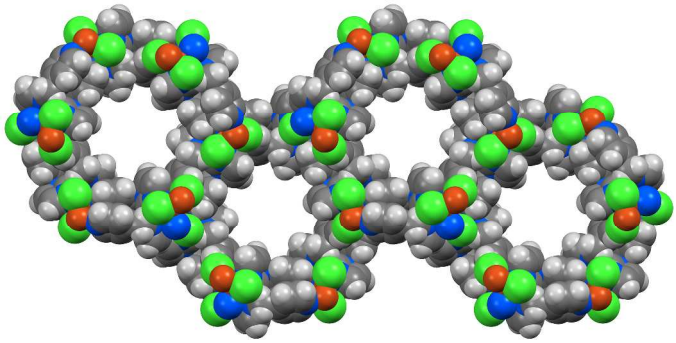

Synopsis

Eight coordination polymers, $\{[Ag(L1)]ClO_4\}_n$ (**1**), $\{[Ag(L2)_{1.5}]ClO_4 \cdot C_2H_3N\}_n$ (**2a**), $\{[Ag(L2)]ClO_4\}_n$ (**2b**), $[Zn(L1)Cl_2]_n$ (**3**), $\{[Zn(L2)Cl_2] \cdot CHCl_3\}_n$ (**4**), $\{[Cu(L1)_2Cl]Cl \cdot H_2O\}_n$ (**5**), $[Cu_2(L2)(\mu\text{-}Cl)_2]_n$ (**6**) and $[Cu_4(L2)(\mu\text{-}Cl)_4]_n$ (**7**) were synthesized *via* self-assembly using semirigid biimidazole derivatives as ligands. The final geometry can be determined by choice of the metal and by adjusting reaction conditions.